The Journal of Experimental Biology **199**, 1115–1126 (1996)
Printed in Great Britain © The Company of Biologists Limited 1996
JEB0211

VOLTAGE- AND Ca^{2+}-GATED CURRENTS IN ZEBRAFISH OLFACTORY RECEPTOR NEURONS

FRANK S. COROTTO, DAVID R. PIPER, NANSHENG CHEN AND WILLIAM C. MICHEL*
Department of Physiology, University of Utah School of Medicine, Salt Lake City, UT 84108, USA

Accepted 23 January 1996

Summary

Voltage- and Ca^{2+}-gated currents were recorded from isolated olfactory receptor neurons (ORNs) of the zebrafish *Danio rerio* using the whole-cell voltage-clamp technique. Zebrafish ORNs had an average capacitance of 0.66 pF and an average apparent input resistance of 8.0 GΩ. Depolarizing steps elicited transient inward currents followed by outward currents with transient and sustained components. The transient inward current (I_{Na}) was sensitive to 1 μmol l^{-1} tetrodotoxin, activated between −74 mV and −64 mV, and reached half-maximal conductance at −28 mV. Its peak amplitude averaged −101 pA. Steady-state inactivation of I_{Na} was half-maximal at an average test potential of −78 mV and recovery from inactivation proceeded with two time constants averaging 23 ms and 532 ms. A sustained, Co^{2+}-sensitive current (I_{Ca}) activated between −44 mV and −34 mV and reached a peak amplitude averaging −9 pA at −14 mV. Outward currents were carried by K^+, based on the reversal potentials of tail currents, and consisted of a Ca^{2+}-dependent K^+ current, a delayed rectifier current (I_{DR}) and a transient K^+ current (I_A). The Ca^{2+}-dependent K^+ current ($I_{K(Ca)}$) activated between −44 mV and −34 mV, whereas I_{DR} and I_A activated between −34 mV and −24 mV. In summary, zebrafish ORNs possess a complement of gated currents similar but not identical to that of ORNs from other vertebrates and which appears well suited for encoding a graded receptor potential into a train of action potentials.

Key words: zebrafish, *Danio rerio*, *Brachydanio rerio*, olfaction, whole-cell currents, patch-clamp.

Introduction

Recently, our understanding of the physiology, biochemistry and molecular biology of olfaction has progressed rapidly. Genes coding for putative olfactory receptor proteins have been cloned (Buck and Axel, 1991; Ngai *et al.* 1993), several transduction pathways have been described (for reviews, see Breer and Boekhoff, 1992; Firestein, 1992; Shepherd, 1994; Zufall *et al.* 1994) and the electrical events that these transduction cascades initiate are becoming better understood (for a review, see Firestein, 1992; see also Miyamoto *et al.* 1992; Dubin and Dionne, 1993; Firestein *et al.* 1993; Ivanova and Caprio, 1993; Kleene, 1993; Kurahashi and Yau, 1993; Lowe and Gold, 1993*a*,*b*; Morales *et al.* 1994; Okada *et al.* 1994). Additional progress in our understanding of olfaction is likely, but may be particularly swift if an animal model is chosen that is particularly useful for genetic analysis. The zebrafish *Danio rerio* is an increasingly popular animal for the study of vertebrate development and its genetic control (Rossant and Hopkins, 1992; Kimmel, 1993; Strähle and Blader, 1994). The characterization of mutants is facilitated because zebrafish are easy to rear and maintain in the laboratory and their embryos develop quickly and externally. Additionally, transgenic zebrafish have been successfully produced (Stuart *et al.* 1990). Recently, the development of the zebrafish olfactory epithelium (Hansen and Zeiske, 1993) and the organization of the olfactory bulb (Baier and Korsching, 1994) have been described and partial gene sequences coding for putative odorant receptors and the locations of receptor cells expressing mRNAs for these receptors have been determined (Byrd *et al.* 1994; Korsching and Baier, 1992; Baier *et al.* 1994).

While these reports constitute significant progress towards a better understanding of olfactory development and differentiation, and may have important implications regarding the encoding of olfactory signals, little is known regarding the physiology of the zebrafish olfactory system. A study employing the underwater electro-olfactogram technique (EOG; Silver *et al.* 1976) has shown that the zebrafish olfactory epithelium responds to a wide range of odorants and is generally similar to that of other fishes in its specificity and sensitivity (Michel and Lubomudrov, 1995). However, it

*Author for correspondence.

remains to be shown that the physiology of single zebrafish olfactory receptor neurons (ORNs) is similar to that of ORNs from other species. Voltage- and Ca^{2+}-activated currents have been described for ORNs from a number of animals and, while there are many similarities between species in their complement of currents, some differences have been noted. For example, ORNs from some species lack transient outward currents while ORNs from others lack inward rectifying currents (see Discussion). To evaluate the usefulness of the zebrafish for the study of olfactory physiology, we have undertaken a study of gated currents in the olfactory receptor cells of the zebrafish. Here we report that zebrafish ORNs possess a complement of voltage- and Ca^{2+}-activated currents similar but not identical to the gated currents reported for ORNs from other species.

Materials and methods

Zebrafish [*Danio rerio*, formerly *Brachydanio rerio* (Hamilton-Buchanan) (Meyer *et al.* 1993)] were purchased from a commercial supplier (Steve Lambourne Co, Inc., Sylmar, CA, USA) and housed in recirculating 40–80 l aquaria at approximately 26 °C. Fish were fed Tetramin flake food daily and used within 6 months of their arrival in the laboratory.

To isolate olfactory rosettes, fish were first immersed in artificial fresh water (see below) containing the general anesthetic MS-222 (20 mg l^{-1}) until gentle pinches to the tail failed to elicit escape behavior. Fish were then rapidly decapitated. Olfactory rosettes were dissected free of the head in cold fish Ringer and kept at 4 °C until needed. Following decapitation, the sex of the fish was determined by opening the abdominal cavity and examining its contents under a dissecting microscope. The presence of oocytes 0.3–0.8 mm in diameter indicated a mature female fish (Selman *et al.* 1993, 1994).

Olfactory receptor neurons (ORNs) were isolated by first placing rosettes in divalent cation-free Ringer containing L-cysteine-activated (1.25 mg ml^{-1}) papain (0.25 mg ml^{-1}) and allowing digestion to occur at room temperature for 15 min. Rosettes were then placed in divalent cation-free Ringer and cells were liberated by trituration onto coverslips coated with concanavalin A.

Whole-cell voltage-clamp recordings were made using borosilicate patch pipettes (resistance approximately 7 MΩ) that had been placed onto ORN somata under visual control. Light suction was applied to achieve a gigaohm seal and greater, maintained suction was applied to achieve the whole-cell configuration. Gated currents were amplified with Axopatch 200 or 200A amplifiers (Axon Instruments, Foster City, CA, USA), low-pass-filtered at 5 kHz (except when recording capacitance transients, see below), digitized on-line, and stored on an IBM-compatible 486 computer using PClamp software. Leak subtraction was performed on-line unless otherwise specified. Data were analyzed using primarily Webfoot software (Salt Lake City, UT, USA) with some analyses performed using Quattro (Borland International, Inc., Scotts Valley, CA, USA).

Cell capacitance (C_m), series resistance (R_s) and input resistance were determined by averaging records obtained from 50 steps from −84 mV to −74 mV (low-pass-filtered at 50 kHz). The difference between the holding currents recorded at these two potentials was noted to calculate input resistance. Capacitance was determined by integrating the area under the averaged capacitance transient to determine net charge. Series resistance was calculated by fitting the decay of the averaged capacitance transient to a single exponential function with time constant τ and applying the formula $R_s=\tau/C_m$. The average R_s value obtained was 36.0±20.0 MΩ (mean ± S.D.). In some cases, on-line R_s compensation was applied at 40–62 %. In cases where large currents were recorded, series resistance error often exceeded 5 mV, so in these cases the magnitude of the error was determined and data were plotted in current–voltage relationships at potentials that had been corrected for this error. Specifically, since every different peak current value that was used to compute a mean current value was actually recorded at a slightly different potential (owing to differences in R_s error), each mean current value was plotted at an average potential that differed by no more than 5 mV from the R_s-corrected potentials at which each of the individual current values were recorded.

Junction potentials between the pipette and bath solutions were measured using a patch pipette filled with 3 mol l^{-1} KCl as the reference electrode (Neher, 1992). These potentials measured +4 mV in magnitude, bath relative to pipette, with both the normal and Cs^+ pipette solutions (see below). All references to membrane potentials have been corrected for the error introduced by junction potentials (Barry and Lynch, 1991).

Equilibrium potentials for ions were calculated with the Nernst equation using concentrations when the concentration of an ion was less than 100 mmol l^{-1} and activities when the concentration was greater than 100 mmol l^{-1}. To determine activities, published values for activity coefficients (Weast, 1968) were fitted to fourth-order polynomial equations and those equations were used to predict the activity coefficients that corresponded to particular ion concentrations through interpolation. Since the activity coefficient of an ion depends on the other ionic species present (Vaughan-Jones and Aikin, 1995), and since we did not attempt to correct for this effect, the resulting calculated equilibrium potentials are only estimates.

Artificial fresh water contained (in mmol l^{-1}): 3.0 NaCl, 0.2 KCl, 0.2 $CaCl_2$, 1.0 Hepes (pH 7.2). Normal fish Ringer (bath solution) contained (in mmol l^{-1}): 137.0 NaCl, 2.0 KCl, 1.8 $CaCl_2$, 1.6 $MgCl_2$, 5.0 Hepes, 10.0 glucose, approximately 4.0 NaOH (pH 7.4). The composition of the divalent-cation-free fish Ringer used in cell dissociation was the same as that of the normal Ringer except that it lacked $CaCl_2$ and $MgCl_2$. In experiments where Ca^{2+} currents were blocked, $CoCl_2$ replaced $CaCl_2$ and $MgCl_2$ in the Ringer's solution on an equimolar basis (Co^{2+} Ringer, 3.4 mmol l^{-1} $CoCl_2$). This

Table 1. *Composition of solutions*

	Ringer	Co^{2+} Ringer	Pipette	Cs^{+} pipette
NaCl	137.0	137.0	–	–
KCl	2.0	2.0	140.0	–
CsCl	–	–	–	140.0
$CaCl_2$	1.8	–	0.1	0.1
$MgCl_2$	1.6	–	2.0	2.0
$CoCl_2$	–	3.4	–	–
Hepes	5.0	5.0	10.0	10.0
Glucose	10.0	10.0	–	–
EGTA	–	–	1.1	1.1
NaOH	approx. 4.0	approx. 4.0	–	approx. 7.7
KOH	–	–	approx. 10.1	–

All concentrations are given in mmol l^{-1}.

allowed us to use the highest possible concentration of $CoCl_2$ while maintaining a normal concentration of divalent cations. In cases where tetrodotoxin (TTX), 4-acetamido-4′-isothiocyanatostilbene-2,2′-disulfonic acid (SITS) or 4-aminopyridine was used, these compounds were added to the Ringer at final concentrations of 1 μmol l^{-1}, 5 mmol l^{-1} and 5 mmol l^{-1}, respectively, without compensation for changes in osmolarity. The composition of the normal pipette solution was (in mmol l^{-1}): 140.0 KCl, 0.1 $CaCl_2$, 2.0 $MgCl_2$, 1.1 EGTA, 10.0 Hepes, approximately 10.1 KOH (pH 7.5). In experiments where K^{+} currents were blocked, the pipette solution contained 140.0 mmol l^{-1} CsCl instead of KCl and approximately 7.7 mmol l^{-1} NaOH instead of KOH (Cs^{+} pipette solution). The free Ca^{2+} concentration in the normal pipette solution was calculated to be 10 nmol l^{-1}. The compositions of the solutions used in this study are summarized in Table 1. All chemicals were obtained from Sigma Chemical Co. (St Louis, MO, USA) or Baxter Diagnostics Inc. (McGaw Park, IL, USA).

Mean values are cited throughout with either the standard deviation (S.D.) or standard error (S.E.M.) where the sample sizes were large and range when the sample sizes were small.

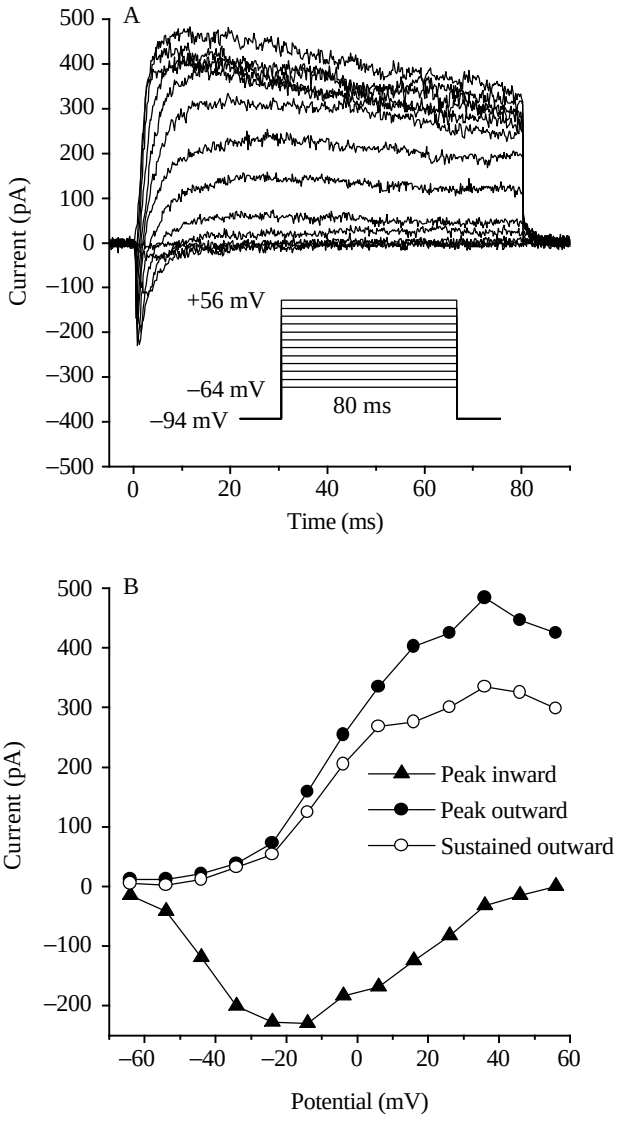

Fig. 1. (A) Total macroscopic currents from one zebrafish olfactory receptor neuron (ORN) subjected to the protocol illustrated. Data were acquired at 5 kHz. (B) Current–voltage relationships of peak inward, peak outward and sustained outward currents from traces shown in A. Normal pipette and Ringer's solution were used.

Results

We report results from 56 zebrafish ORNs. Olfactory receptor neurons appeared as round somata with diameters of approximately 4 μm and possessing a single thick process of approximately 2 μm in diameter and of 6–15 μm in length (the dendrite). Apical cilia were evident on approximately 10 % of these dendrites. Twenty-three per cent of the cells (13 out of 56) also possessed a much thinner process of variable length (but generally less than 10 μm) which was presumably the axon. Upon achieving the whole-cell recording configuration, all cells assumed a rounded morphology. The average cell capacitance was 0.66±0.18 pF (S.D.) and the average apparent input resistance was 8.0±7.5 GΩ (S.D.). With normal Ringer and pipette solution, depolarizing steps from a holding potential of −94 mV elicited a rapid, transient inward current followed by outward currents with transient and sustained components (Fig. 1). Presumably as a result of the small cell size and rounded morphology during recording, we saw no evidence of poor voltage control due to space-clamp problems.

Transient inward current

The transient inward current was isolated using the Cs^{+} pipette solution and Co^{2+} Ringer in the bath. Depolarizing steps elicited transient inward currents that first activated between −74 mV and −64 mV (15 cells; Fig. 2A). Current amplitude increased with further depolarization to about −20 mV and then decreased at more positive test potentials. The peak transient inward current ranged from −15 to −307 pA and occurred at test potentials ranging from −24 to

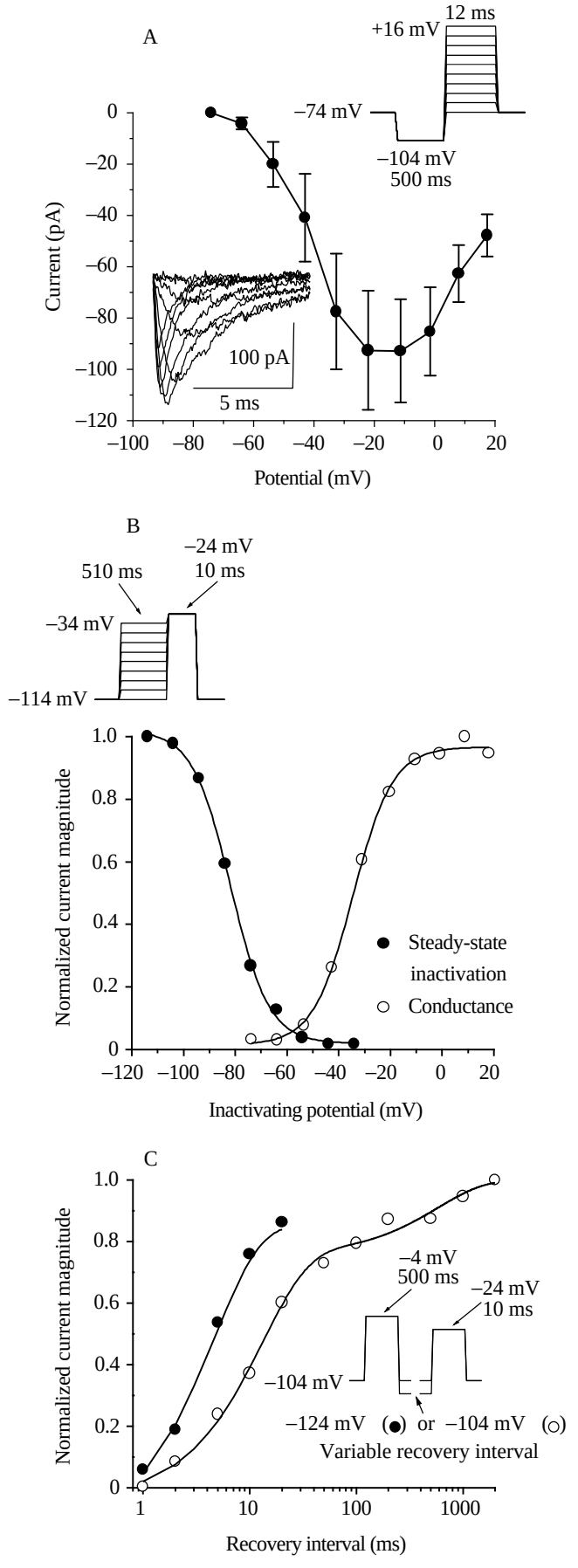

Fig. 2. Properties of I_{Na} in zebrafish ORNs. Currents were isolated with Co^{2+} Ringer and the Cs^+ pipette solution. (A) Average peak Na^+ currents (I_{Na}) from 15 zebrafish ORNs (except at −43 mV, +8 mV and +17 mV, where 14 cells were used) subjected to the protocol illustrated. Data were acquired at 20 kHz at test potentials. Test potentials were corrected off-line for series resistance (R_s) error and the data are plotted at these corrected potentials. Error bars denote standard error of the mean. Inset: representative traces from one cell. (B) The voltage-dependence of the Na^+ conductance (G_{Na}) from one zebrafish ORN and steady-state inactivation of I_{Na} from another ORN. Conductance was determined by applying Ohm's law to I_{Na} recorded at various membrane potentials with the use of a routine that both corrected for series resistance error and allowed the reversal potential to float to obtain the best fit to the Boltzman equation. In this example, half-maximal G_{Na} was at −35 mV and the predicted reversal potential was +62 mV. For determining steady-state inactivation, cells were subjected to the protocol illustrated. Data were acquired at 50 kHz during the step to −24 mV. Plotted are peak magnitudes of I_{Na} elicited following inactivating steps (to potentials on the abscissa) normalized to the peak magnitude of I_{Na} observed after holding the cell at −114 mV. The curve shown was obtained by fitting the data to the Boltzman equation. On the basis of this fit, half-maximal inactivation in this example was determined to be at −82 mV. (C) Recovery of I_{Na} from inactivation in one representative zebrafish ORN subjected to the protocol illustrated. Data were acquired at 50 kHz during the step to −24 mV. Plotted are peak magnitudes of I_{Na} elicited after recovery intervals shown on the abscissa relative to the maximum I_{Na} evoked from this cell (which was after 2 s at −104 mV). In this cell, recovery at −104 mV occurred with time constants of 13 and 582 ms. Recovery was much faster at −124 mV, but long recovery periods at this potential caused seal degradation and subsequent loss of recordings. Lines were obtained by fitting data to double (−104 mV) and single (−124 mV) exponential functions.

−4 mV. For each of these cells, current amplitudes were converted to conductance measurements using a routine that corrected the membrane potentials for the error introduced by the series resistance and allowed the reversal potential to float to achieve the best fit to the Boltzman function. Using this method, the average potential where conductance was half-maximal was determined to be −28±11 mV (S.D.) and the average predicted reversal potential was determined to be +57±22 mV (S.D.; Fig. 2B). We conclude that this current is a Na^+ current (I_{Na}) in part because this value for the average reversal potential is close to the estimated value of E_{Na} (which is +67 mV) but also because the current was never observed when the bath contained TTX and because the current was insensitive to the Co^{2+} in the Co^{2+} Ringer.

With I_{Na} isolated using the agents described above, the voltage-dependence of its steady-state inactivation was determined in four cells by first holding cells at −114 mV and then stepping to various potentials to achieve steady-state inactivation of I_{Na} followed by a step to −24 mV to elicit the residual I_{Na} that had not been inactivated. The resulting data were fitted with a Boltzman distribution and the subsequent fits were used to determine the potential at which inactivation was half-maximal (Fig. 2B). The average potential for half-maximal inactivation was −78 mV (range −69 to −82 mV).

With I_{Na} isolated as above, recovery of I_{Na} from inactivation was investigated in eight zebrafish ORNs by holding cells at −104 mV, stepping to −4 mV to inactivate I_{Na} completely, stepping back to −104 mV for various times to allow some degree of recovery, and finally stepping to −24 mV to elicit I_{Na}. The resulting current magnitudes were plotted as a function of the recovery interval and were fitted well by double exponential functions (Fig. 2C). At −104 mV, the average time constants of recovery were 23±21 ms and 532±474 ms (S.D.). Recovery was much faster at −124 mV (two cells; Fig. 2C), but it was not possible to hold cells for the full duration of an experiment at this potential. This made it impossible to obtain accurate measurements of the second, slower time constant of recovery but the faster time constants were 7 ms and 5 ms in these two cells.

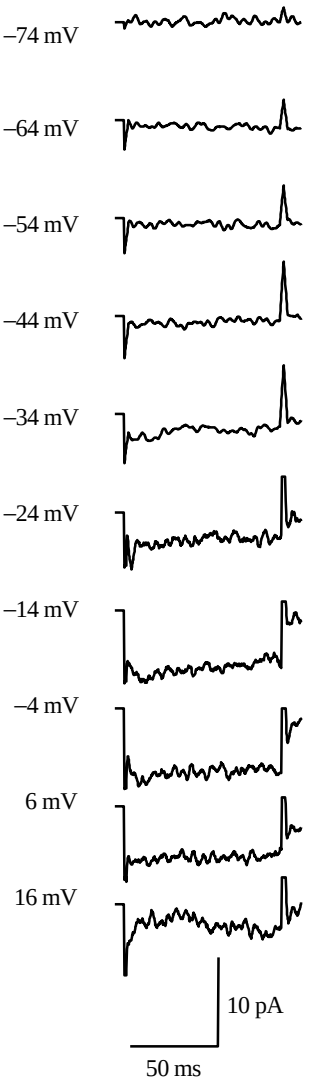

Fig. 3. Ca^{2+} currents from one zebrafish ORN. Traces are offset for clarity. Cells were held at −94 mV and stepped to the test potentials shown for 90 ms. Data were acquired at 10 kHz. Leak substraction was applied to the traces. Ca^{2+} currents were recorded with normal Ringer containing 1 μmol l^{-1} tetrodotoxin (TTX) bathing the cell and the Cs^{+} pipette solution. The Ca^{2+} current was subsequently blocked when the bath solution was switched to Co^{2+} Ringer with TTX (not shown). To reduce noise, each trace was obtained by averaging the data from four such steps and then each averaged trace was smoothed by performing a running 11-point average. This procedure eliminated the short period of each trace recorded before each step, so baseline data were added afterwards to provide an indication of the zero-current baseline. Capacitance transients have been truncated.

Sustained inward current

A sustained inward current was investigated in four cells by including TTX in the Ringer and using the Cs^{+}-based pipette solution. Depolarizing steps from a holding potential of −94 mV elicited a very small inward current that in three cells appeared to be sustained except at +16 mV (Fig. 3), while in a fourth cell the inward current appeared to be transient at all potentials. Because this current was highly labile, it was not possible to demonstrate its Co^{2+}-sensitivity by first observing the current, then blocking it with Co^{2+} Ringer, and then showing recovery in normal Ringer. Therefore, in two of these cells, the current was first observed in normal Ringer (with TTX) and then blocked by changing the bath to Co^{2+} Ringer (with TTX), while in the other two cells this order of bath presentation was reversed. Results were similar with either order of bath presentation. A very small Co^{2+}-sensitive current, which was presumably I_{Ca}, was activated between −44 and −34 mV (Fig. 4). Its amplitude increased at more positive potentials to reach a peak at approximately −10 mV and then declined at still more positive potentials. In the one cell where this current appeared transient at all potentials, contaminating currents were observed in the presence of Co^{2+} Ringer. When contaminating currents were removed by subtracting them

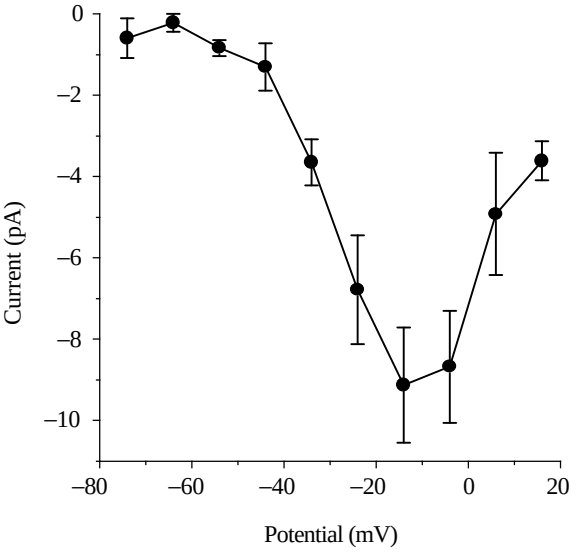

Fig. 4. Average peak Ca^{2+} currents (I_{Ca}) from four zebrafish ORNs determined at various test potentials. Cells were subjected to the protocol described for Fig. 3. For each cell, data from four such protocols were averaged to reduce noise. Peak current values were determined from these averaged traces. Error bars denote standard error of the mean.

from the currents originally observed in normal Ringer (with 1 μmol l^{-1} TTX), the isolated Co^{2+}-sensitive I_{Ca} was found to be largely sustained (not shown). Therefore, the transient nature of the currents originally observed in this cell was due to the presence of contaminating currents. In contrast, the transient nature of I_{Ca} at +16 mV was observed in all cells examined (Fig. 4) and was not due to contamination as blocking I_{Ca} with Co^{2+} Ringer did not reveal contaminating currents. In three other cells where contaminating currents were observed, they were unaffected by changing the bath to Ringer containing the Cl^- channel blocker SITS (5 mmol l^{-1}), so it is unlikely that these currents were carried by Cl^-.

Outward currents

Ca^{2+}-independent outward currents were elicited from eight cells by applying depolarizing steps using the normal pipette solution and with Co^{2+} Ringer containing TTX in the bath. In five of these eight cells, depolarizing steps were also applied with normal Ringer (with TTX) in the bath to elicit total outward currents and the Ca^{2+}-dependent component was isolated by subtracting traces obtained with Co^{2+} Ringer from those obtained with normal Ringer. Ca^{2+}-independent outward currents appeared first between −34 and −24 mV and increased at more positive potentials (Fig. 5B,D). Ca^{2+}-dependent outward currents were first measurable between −44 and −34 mV, reached a peak at approximately 0 mV, and declined at more positive potentials (Fig. 5C,D). Both Ca^{2+}-dependent and Ca^{2+}-independent outward currents displayed inactivation.

The ion-carrying outward current was determined by analyzing tail currents. With Ca^{2+}-independent outward currents isolated as described above, seven cells were first held at −74 mV, then stepped to +16 mV to activate outward currents, and finally stepped to test potentials ranging from −134 to −94 mV to elicit tail currents (Fig. 6). The average reversal potential of the Ca^{2+}-independent outward currents was −116 mV (range −127 to −107 mV), which is near the estimated value for E_K of −107 mV. In two cells, the reversal potential of the Ca^{2+}-dependent outward current was

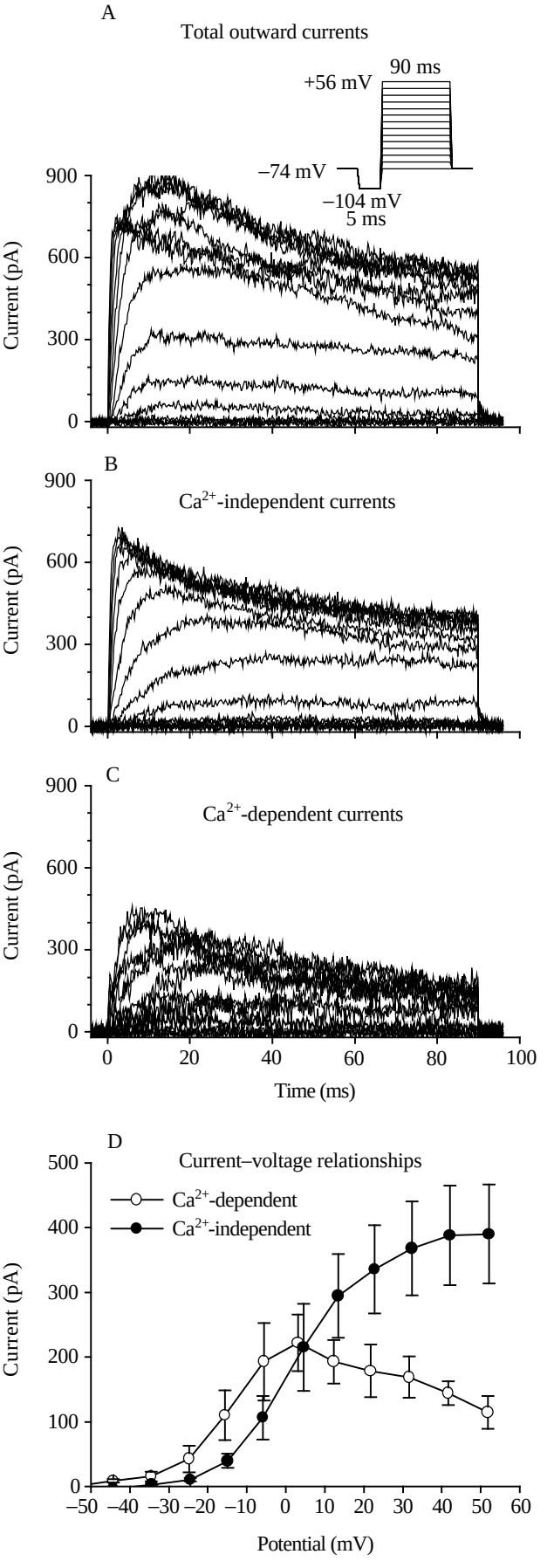

Fig. 5. Outward currents from zebrafish ORNs consist of both Ca^{2+}-independent and Ca^{2+}-dependent currents. (A) Total outward currents recorded at various test potentials from one zebrafish ORN subjected to the protocol illustrated. Total outward currents were isolated by including 1 μmol l^{-1} TTX in the bath. (B) Ca^{2+}-independent outward currents recorded from the same cell as in A, and subjected to the same protocol, but with I_{Ca} and $I_{K(Ca)}$ blocked by replacing the bath with Co^{2+} Ringer containing TTX. (C) Ca^{2+}-dependent outward currents obtained by subtracting traces in B from traces in A. (D) Average peak Ca^{2+}-independent (eight cells) and Ca^{2+}-dependent (five cells) outward currents at various membrane potentials. Data were obtained as described in A–C. Test potentials were corrected off-line for R_s error and the data are plotted at these corrected potentials. Error bars denote standard error of the mean. Currents shown in A and C, and the Ca^{2+}-dependent currents shown in D, were presumably contaminated by I_{Ca}. The magnitude of this contaminating current was negligible (see Fig. 4). All data were acquired at 10 kHz.

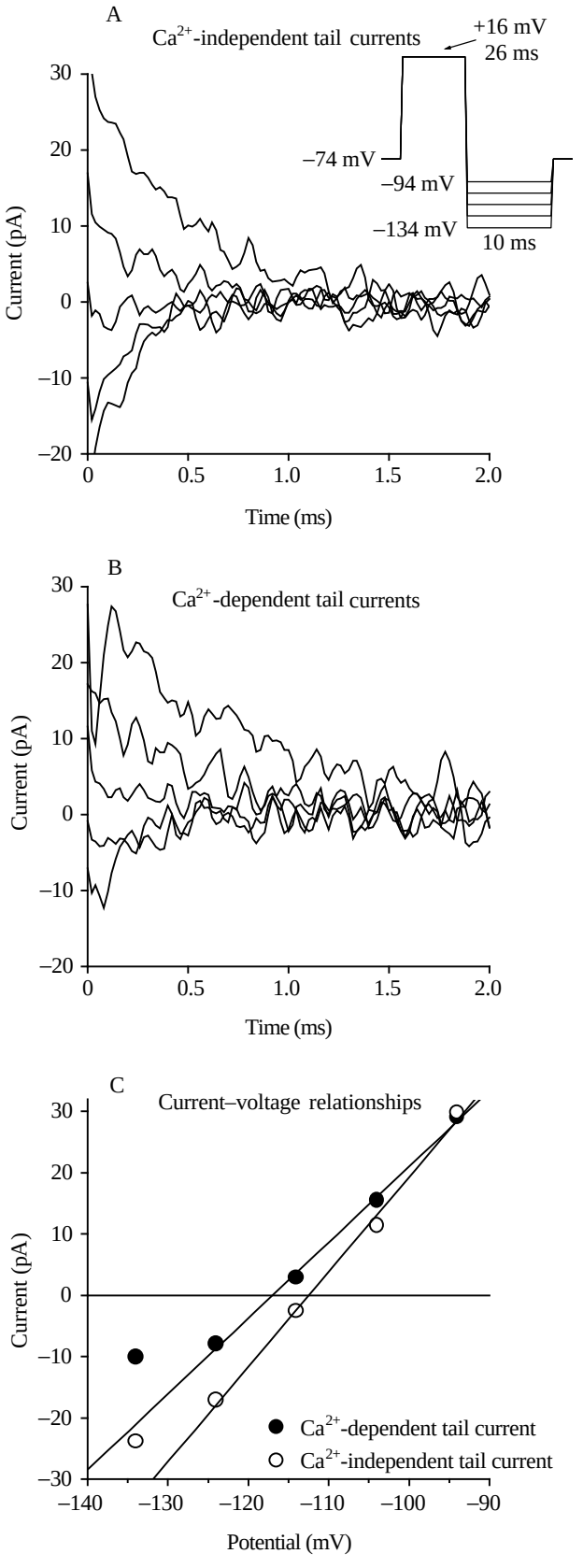

Fig. 6. Outward currents are carried by K^+. (A) Ca^{2+}-independent tail currents recorded from one cell subjected to the protocol illustrated using the normal pipette solution and Co^{2+} Ringer with 1 μmol l^{-1} TTX. Data were acquired at 50 kHz during steps to test potentials (also in B). To reduce noise, each trace was obtained by averaging data from four steps to test potentials. Tail currents were fitted to single exponential functions and these functions were used to predict the current magnitude at the onset of the step. These predicted current magnitudes were used to determine reversal potentials as in C. (B) Ca^{2+}-dependent tail currents obtained from a different cell from the one shown in A. Data were obtained as in A except that tail currents were first recorded with normal Ringer (with TTX) and then with Co^{2+} Ringer (with TTX). The Ca^{2+}-dependent tail currents shown were obtained by subtraction. (C) Instantaneous current–voltage relationships of tail current magnitudes predicted from traces shown in A and B. Linear regression was used to determine the reversal potentials of these tail currents. Current magnitudes at −134 mV were not included in the regressions because the tail currents displayed outward rectification. In these examples, the predicted reversal potential of the Ca^{2+}-independent tail current was −113 mV and that of the Ca^{2+}-dependent tail current was −117 mV.

determined by first eliciting total tail currents using normal Ringer with TTX and then again with Ca^{2+}-dependent currents blocked (using Co^{2+} Ringer with TTX). In a third cell, the order of bath presentations was reversed. Subtraction yielded Ca^{2+}-dependent tail currents. The average reversal potential of the Ca^{2+}-dependent tail currents was −102 mV (range −117 to −85 mV; Fig. 6) which is close to the estimated value of E_K of −107 mV. Since the estimated value for E_{Cl} is −1 mV, it is clear that the Ca^{2+}-dependent outward currents were carried largely by K^+ and not by Cl^-.

To determine whether the Ca^{2+}-independent K^+ current consisted of a single inactivating current or an inactivating current (such as an A-current; I_A) and a delayed rectifier current (I_{DR}), Ca^{2+}-independent outward currents were isolated from eight cells using the agents described above and then cells were subjected first to a protocol that elicited total Ca^{2+}-independent outward currents and then to a protocol that inactivated I_A and selectively activated I_{DR}. To elicit total Ca^{2+}-independent outward currents, cells were held at −74 mV and then stepped to −124 mV to remove any steady-state inactivation, and finally stepped to various test potentials (Fig. 7A). To elicit the delayed rectifier current selectively, cells were subjected to the same protocol but, instead of being stepped to −124 mV, they were stepped to −44 mV to inactivate I_A (Fig. 7B). Subtraction yielded the current inactivated at −44 mV (Fig. 7C). Results are consistent with the presence of two Ca^{2+}-independent K^+ currents, I_A and I_{DR}. Both currents activated between −34 and −24 mV and increased in magnitude with further depolarization (Fig. 7D). The observation that isolated I_{DR} displayed some inactivation (Fig. 7B) suggests that the two currents were not completely separated by this method; I_A was probably not completely inactivated at −44 mV. Therefore, the rate of I_A inactivation was determined by fitting total Ca^{2+}-independent K^+ current traces (e.g. Fig. 7A) rather than fitting traces of isolated I_A. At approximately 40 mV (the value varied slightly owing to differences between cells in series resistance error), the rate of

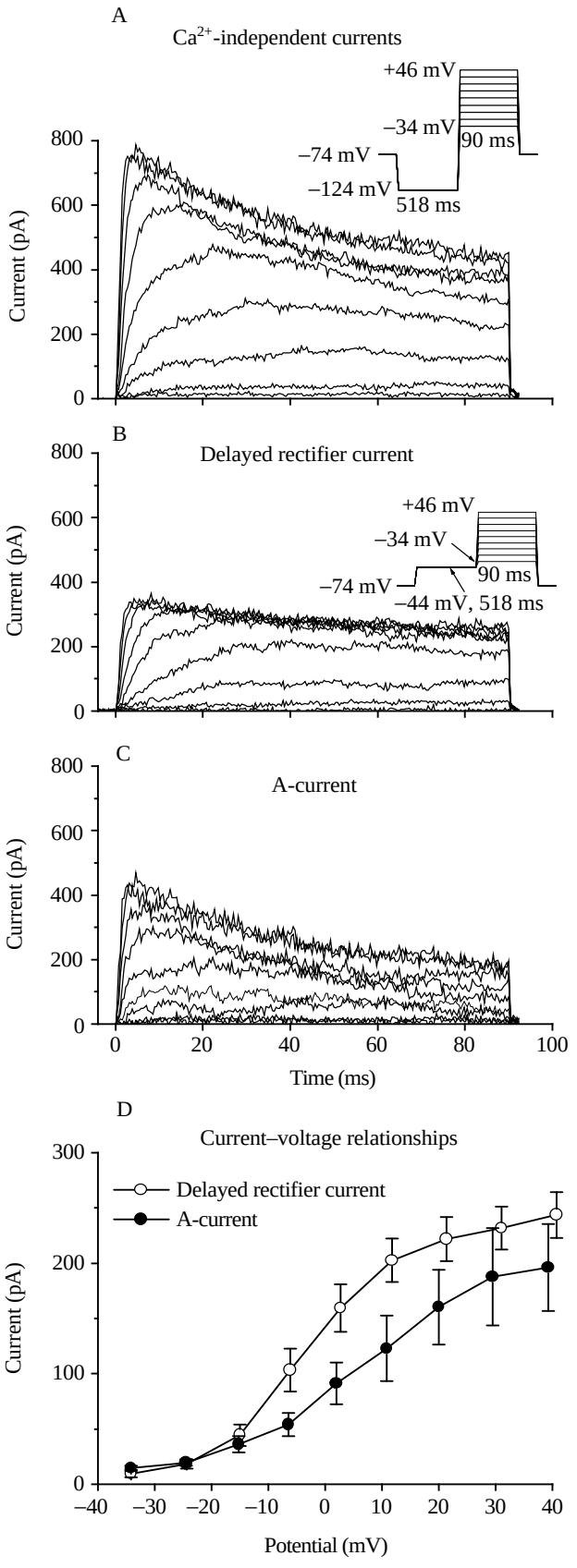

Fig. 7. Ca^{2+}-independent outward currents from zebrafish ORNs consist of both delayed rectifier and A-currents (I_A). (A) Ca^{2+}-independent outward currents recorded from a zebrafish ORN were subjected to the protocol illustrated. Currents were isolated using Co^{2+} Ringer with TTX and the normal pipette solution. Traces were recorded without leak subtraction. (B) Delayed rectifier currents recorded from the same cell and subjected to the protocol illustrated which inactivated I_A by holding the cell at −44 mV. Traces were recorded without leak subtraction. Data in A and B were acquired at 2.6 kHz. (C) I_A obtained by subtracting traces in B from traces in A. This subtraction procedure also removed leak currents. (D) Average peak Ca^{2+}-independent outward currents at various membrane potentials from five zebrafish ORNs. Data were obtained as described in A–C. The test potentials were corrected off-line for R_s error and the data are plotted at these corrected potentials. Leak currents were subtracted off-line prior to determining peak I_{DR}. Error bars denote standard error of the mean.

inactivation was best fitted by a single exponential function with an average time constant of 76±57 ms (eight cells, S.D.). This is similar to values reported for I_A in other systems (Rudy, 1988). Inactivation was not analyzed at other potentials, but inspection of current traces (e.g. Fig. 7A) suggests that this rate of inactivation was independent of membrane potential.

In some neurons, I_A can be discriminated from I_{DR} pharmacologically using 4-aminopyridine (4-AP; Hille, 1992). To determine whether I_A in zebrafish ORNs is 4-AP-sensitive, total Ca^{2+}-independent currents were recorded from four ORNs before and during exposure to 5 mmol l^{-1} 4-AP. Subtraction of the relatively sustained 4-AP-insensitive current (I_{DR}, Fig. 8B) from the total Ca^{2+}-independent outward current (Fig. 8A) left a rapidly inactivating 4-AP-sensitive outward current (I_A, Fig. 8C).

Hyperpolarization-activated currents

To determine whether zebrafish ORNs possessed currents activated by hyperpolarization, six cells were held at −54 mV and stepped to potentials ranging from −69 to −129 mV for 875 ms. One of these cells displayed slow, inward rectification (not shown) but the others did not. Hyperpolarization-activated currents were also not observed in the eight cells described above that had been stepped from −74 to −124 mV for 518 ms in experiments designed to separate I_A from I_{DR}. Inward rectifying currents were not investigated further.

Michel and Lubomudrov (1995) have reported sex differences in olfactory sensitivity of zebrafish using the EOG technique. With the limited number of cells in this study, we found no obvious sex differences in the magnitudes or thresholds of gated currents. This is consistent with the belief that voltage- and Ca^{2+}-gated currents do not contribute to the EOG, which reflects instead the summed receptor potentials of many ORNs (Getchell, 1986).

Discussion

We have characterized five gated currents in zebrafish ORNs: a transient TTX-sensitive I_{Na}, a sustained I_{Ca}, I_{DR}, a Ca^{2+}-dependent K^+ current ($I_{K(Ca)}$) and I_A. The I_{Na} found in zebrafish ORNs appears to be generally similar to that found

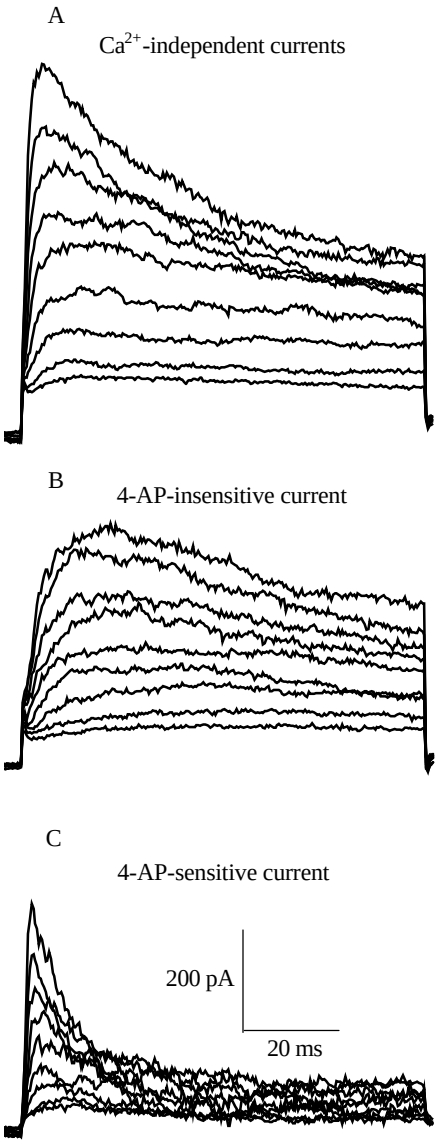

Fig. 8. The rapidly inactivating component of the Ca^{2+}-independent outward current is sensitive to 4-aminopyridine (4-AP). (A) Ca^{2+}-independent outward currents recorded from a zebrafish ORN subjected to the voltage protocol illustrated in Fig. 7A. Currents were isolated using Co^{2+} Ringer with TTX and the normal pipette solution. Traces were recorded without leak subtraction. (B) The 4-AP-insensitive currents (I_{DR}) were recorded using the same protocol as in A but with 5 mmol l^{-1} 4-AP added to the Ringer. Traces were recorded without leak subtraction. Data in A and B were acquired at 2.6 kHz. (C) The 4-AP-sensitive current (I_A) was obtained by subtracting traces in B from traces in A. This subtraction procedure also removed leak currents.

in other species. The current is activated first between −74 and −64 mV (Fig. 2A), and similar thresholds have been reported for ORNs from *Xenopus laevis* (Schild, 1989), rat (Rajendra *et al.* 1992; Murrow *et al.* 1995) and catfish (Miyamoto *et al.* 1992). Others have reported more positive thresholds (Trotier, 1986; Firestein and Werblin, 1987; McClintock and Ache, 1989; Suzuki, 1989; Trombley and Westbrook, 1991; Zufall *et al.* 1991; Lucero *et al.* 1992; Nevitt and Moody, 1992; Delgado and Labarca, 1993). The fact that, while in the gigaseal cell-attached configuration, we only rarely observed action potentials indicates that the resting membrane potential of zebrafish ORNs may be more negative than spike threshold, i.e. more negative than −74 to −64 mV. Another possibility is that the resting membrane potential is sufficiently positive that Na^+ channels are inactivated at rest. It was not possible to measure the membrane potential directly because of problems inherent in the study of such small cells; the seal conductance contributes significantly to the resting conductance of the cell, leading to erroneous determinations of both membrane potential and input resistance (Barry and Lynch, 1991).

Recovery of I_{Na} from inactivation was very slow in zebrafish ORNs (Fig. 2C). Similar results have been reported for rat ORNs (Rajendra *et al.* 1992), and in ORNs from both species the rate of recovery from inactivation is voltage-dependent, being much faster at more negative potentials. Slow recovery has also been reported in salmon ORNs while, in contrast, recovery from inactivation is relatively rapid in ORNs from catfish (Miyamoto *et al.* 1992) and lobster (McClintock and Ache, 1989). Slow recovery from inactivation could profoundly affect firing properties by causing progressive spike amplitude decrement and spike frequency adaptation. Spike amplitude decrement during firing has been reported for ORNs from a large number of species using whole-cell, conventional intracellular, and extracellular recording techniques (Suzuki, 1977, 1989; Trotier and MacLeod, 1986; Firestein and Werblin, 1987; Firestein *et al.* 1990; Frings and Lindemann, 1991).

The extremely small I_{Ca} that we observed in zebrafish ORNs is activated at a threshold between −44 and −34 mV (Fig. 4) and appears to be largely sustained except at +16 mV (Fig. 3). By recording four steps to each test potential, averaging each of the four steps and smoothing the resulting data, we were able to detect I_{Ca} in zebrafish ORNs that usually measured less than −10 pA in peak amplitude. It is difficult to compare our results with those of others because of the common practice of increasing the extracellular Ca^{2+} concentration, or adding Ba^{2+} to the bath, to increase the amplitude of the currents observed. Since this practice usually results in an increase in the extracellular concentration of divalent cations, it would be expected to shift the voltage-dependence towards more positive potentials (Hille, 1992). In some ORNs that have been studied using normal divalent cation concentrations, thresholds for I_{Ca} activation were found to be around −20 mV (Firestein and Werblin, 1987; Suzuki, 1989; Delgado and Labarca, 1993), which is more positive than we found in zebrafish ORNs. However, in lobster and salmon ORNs (McClintock and Ache, 1989; Nevitt and Moody, 1992), I_{Ca} threshold was more negative, ranging from −40 to −30 mV. Because the threshold of I_{Ca} activation in zebrafish ORNs is intermediate between that described for low-threshold (T-type, thresholds between −65 and −50 mV) and high-threshold (L- and N-type, thresholds positive from −10 mV) Ca^{2+} currents (see Tsien *et al.* 1988, for a review), we cannot group the I_{Ca} that we

describe into any of these categories without further study, such as testing for dihydropyridine-sensitivity. It may be that I_{Ca} in zebrafish ORNs is passed by several different channel types or, alternatively, that I_{Ca} does not fit into any of these categories; this is certainly true for some other Ca^{2+} currents that have been described (Tsien *et al.* 1988).

We describe three outward K^+ currents: I_{DR}, $I_{K(Ca)}$ and I_A (Figs 5–7). In general, these currents are found in ORNs from other species as well. Exceptions include ORNs from lobster (McClintock and Ache, 1989), neonatal rat (Trombley and Westbrook, 1991) and the toad *Caudiverbera caudiverbera* (Delgado and Labarca, 1993), which lack transient outward currents. We characterize the transient outward current that we describe as an A-current largely on the basis of its sensitivity to 4-aminopyridine and its inactivation rate; the average time constant at +40 mV is 76 ms, which is well within the range of A-currents described in other species (Rudy, 1988). It is likely that I_A in zebrafish ORNs plays roles similar to those described in other cells, such as delaying the onset to the first spike, lengthening the interspike interval (Hille, 1992) or assisting in spike repolarization (Sacchi and Belluzzi, 1993).

We failed to demonstrate the existence of a Ca^{2+}-dependent Cl^- current ($I_{Cl(Ca)}$) in zebrafish ORNs. A Ca^{2+}-dependent Cl^--current would have been evident in two sets of experiments. First, when I_{Ca} was isolated, $I_{Cl(Ca)}$ would have led to the development of small outward currents at +16 mV. Outward currents were occasionally observed under these conditions but these currents could not be blocked by replacing the bath with Co^{2+} Ringer, so they were not Ca^{2+}-dependent, and they were not blocked by SITS, so they were probably not carried by Cl^-. Second, $I_{Cl(Ca)}$ should have caused the reversal potential of the Ca^{2+}-dependent outward currents to be well positive of E_K since the estimated value of E_{Cl} is −1 mV. In one cell, the Ca^{2+}-dependent tail currents reversed at −85 mV, which suggests that the tail currents were not carried exclusively by K^+. Obviously Ca^{2+} is a potential current carrier in this case, in addition to Cl^-. In the other two cells examined, the Ca^{2+}-dependent tail currents reversed quite close to E_K. Ca^{2+}-dependent Cl^- currents have recently been described in ORNs from other species, where they participate in generating the receptor potential (Kleene, 1993; Kurahashi and Yau, 1993; Lowe and Gold, 1993*a*). It is likely that a Cl^- current plays a similar role in zebrafish ORNs because EOG recordings have shown that odor responses can be markedly reduced by application of the Cl^- channel blocker SITS (W. C. Michel, unpublished observations). Our failure to demonstrate the presence of a Ca^{2+}-dependent Cl^- conductance could have resulted from the loss of cilia during the dissociation procedure if this conductance is found exclusively on the cilia. Approximately 10 % of the cells used in the present study had obvious cilia. Another possibility is that the cilia lack a voltage-gated Ca^{2+} current and so depolarizing voltage steps would not be expected to activate an exclusively ciliary $I_{Cl(Ca)}$.

The voltage- and Ca^{2+}-activated currents that we describe appear well suited for encoding a graded receptor potential into a train of action potentials. The Ca^{2+} current is probably too small to contribute significantly to generating the action potential but, by gating $I_{K(Ca)}$, probably contributes to spike repolarization and perhaps spike frequency adaptation. The A-current may assist in spike repolarization and probably lengthens the interspike interval to allow encoding of a broader range of receptor potential amplitudes than would be possible otherwise. The general absence of inward rectifying currents suggests that the resting membrane potential is set by the equilibrium potential of leak currents rather than resulting from a balance of leak and inward rectifying currents as is found in some other cells (Hille, 1992).

With the emergence of the zebrafish as an important model for investigations of the molecular basis of olfactory development, it becomes increasingly important to characterize the olfactory capabilities of this species functionally. Behavioral studies have shown that zebrafish respond to chemosensory stimuli; both amino acids and putative pheromones elicit behavioral responses (Bloom and Perlmutter, 1977; Van Den Hurk and Lambert, 1983; Van Den Hurk *et al.* 1987; Steele *et al.* 1990, 1991). Michel and Lubomudrov (1995) have recently shown that the zebrafish olfactory organ has a response specificity similar to that of most other fishes. The current investigation demonstrates that isolated zebrafish ORNs are amenable to electrophysiological characterization. High-resistance seals formed easily and, in 25 % of the cells studied, a seal resistance greater than 20 GΩ (measured as input resistance) was maintained after achieving the whole-cell configuration. The small size of zebrafish ORNs allows for excellent voltage control and for rapid perfusion of the cell with the pipette solution in the whole-cell configuration. Rapid perfusion should allow efficient targeting of biochemical probes to transduction sites in the cilia of ORNs. All of these factors suggest that zebrafish ORNs have particular advantages for the study of olfactory physiology.

We thank Dr Mary T. Lucero for a critical reading of an earlier version of this manuscript. This work was supported by NIDCD DC-01418.

References

BAIER, H. AND KORSCHING, S. (1994). Olfactory glomeruli in the zebrafish form an invariant pattern and are identifiable across animals. *J. Neurosci.* **14**, 219–230.

BAIER, H., ROTTER, S. AND KORSCHING, S. (1994). Connectional topography in the zebrafish olfactory system: Random positions but regular spacing of sensory neurons projecting to an individual glomerulus. *Proc. natn. Acad. Sci. U.S.A.* **91**, 11646–11650.

BARRY, P. H. AND LYNCH, J. W. (1991). Liquid junction potentials and small cell effects in patch-clamp analysis. *J. Membr. Biol.* **121**, 101–117.

BLOOM, H. D. AND PERLMUTTER, A. (1977). A sexual aggregating pheromone system in the zebrafish, *Brachydanio rerio* (Hamilton-Buchanan). *J. exp. Zool.* **199**, 215–226.

BREER, H. AND BOEKHOFF, I. (1992). Second messenger signalling in olfaction. *Curr. Opin. Neurobiol.* **2**, 439–443.

BUCK, L. AND AXEL, R. (1991). A novel multigene family may encode odorant receptors: A molecular basis for odor recognition. *Cell* **65**, 175–187.

BYRD, C. A., VOGT, R. G. AND BRUNJES, P. C. (1994). Expression of odorant receptor proteins during post-embryonic development in zebrafish. *Chem. Senses* (Abstract) **19**, 448–449.

DELGADO, R. AND LABARCA, P. (1993). Properties of whole cell currents in isolated olfactory neurons from the chilean toad *Caudiverbera caudiverbera*. *Am. J. Physiol.* **264**, C1418–C1427.

DUBIN, A. E. AND DIONNE, V. E. (1993). Modulation of Cl^-, K^+ and nonselective cation conductances by taurine in olfactory receptor neurons of the mudpuppy *Necturus maculosus*. *J. gen. Physiol.* **101**, 469–485.

FIRESTEIN, S. (1992). Electrical signals in olfactory transduction. *Curr. Opin. Neurobiol.* **2**, 444–448.

FIRESTEIN, S., PICCO, C. AND MENINI, A. (1993). The relation between stimulus and response in olfactory receptor cells of the tiger salamander. *J. Physiol., Lond.* **468**, 1–10.

FIRESTEIN, S., SHEPHERD, G. M. AND WERBLIN, F. S. (1990). Time course of the membrane current underlying sensory transduction in salamander olfactory receptor neurones. *J. Physiol., Lond.* **430**, 135–158.

FIRESTEIN, S. AND WERBLIN, F. S. (1987). Gated currents in isolated olfactory receptor neurons of the larval tiger salamander. *Proc. natn. Acad. Sci. U.S.A.* **84**, 6292–6296.

FRINGS, S. AND LINDEMANN, B. (1991). Current recording from sensory cilia of olfactory receptor cells *in situ*. I. The neuronal response to cyclic nucleotides. *J. gen. Physiol.* **97**, 1–16.

GETCHELL, T. V. (1986). Functional properties of vertebrate olfactory receptor neurons. *Physiol. Rev.* **66**, 772–818.

HANSEN, A. AND ZEISKE, E. (1993). Development of the olfactory organ in the zebrafish, *Brachydanio rerio*. *J. comp. Neurol.* **333**, 289–300.

HILLE, B. (1992). *Ionic Channels of Excitable Membranes*. Sunderland, MA: Sinauer Assoc., Inc.

IVANOVA, T. T. AND CAPRIO, J. (1993). Odorant receptors activated by amino acids in sensory neurons of the channel catfish *Ictalurus punctatus*. *J. gen. Physiol.* **102**, 1085–1105.

KIMMEL, C. B. (1993). Patterning the brain of the zebrafish embryo. *A. Rev. Neurosci.* **16**, 707–732.

KLEENE, S. J. (1993). Origin of the chloride current in olfactory transduction. *Neuron* **11**, 123–132.

KORSCHING, S. AND BAIER, H. (1992). Towards a coding strategy in the fish olfactory system. *Chem. Senses* **17** (Abstract), 653.

KURAHASHI, T. AND YAU, K.-W. (1993). Co-existence of cationic and chloride components in odorant-induced current of vertebrate olfactory receptor cells. *Nature* **363**, 71–74.

LOWE, G. AND GOLD, G. H. (1993*a*). Nonlinear amplification by calcium-dependent chloride channels in olfactory receptor cells. *Nature* **366**, 283–286.

LOWE, G. AND GOLD, G. H. (1993*b*). Contribution of the ciliary cyclic nucleotide-gated conductance to olfactory transduction in the salamander. *J. Physiol., Lond.* **462**, 175–196.

LUCERO, M. T., HORRIGAN, F. T. AND GILLY, W. F. (1992). Electrical responses to chemical stimulation of squid olfactory receptor cells. *J. exp. Biol.* **162**, 231–249.

MCCLINTOCK, T. S. AND ACHE, B. W. (1989). Ionic currents and ion channels of lobster olfactory receptor neurons. *J. gen. Physiol.* **94**, 1085–1099.

MEYER, A., BIERMANN, C.H. AND ORTI, G. (1993). The phylogenetic position of the zebrafish (*Danio rerio*), a model system in developmental biology: An invitation to the comparative method. *Proc. R. Soc. Lond. B* **252**, 231–236.

MICHEL, W. C. AND LUBOMUDROV, L. M. (1995). Specificity and sensitivity of the olfactory organ of the zebrafish, *Danio rerio*. *J. comp. Physiol.* A **177**, 191–199.

MIYAMOTO, T., RESTREPO, D. AND TEETER, J. H. (1992). Voltage-dependent and odorant-regulated currents in isolated olfactory receptor neurons of the channel catfish. *J. gen. Physiol.* **99**, 5095–5530.

MORALES, B., UGARTE, G., LABARCA, P. AND BACIGALUPO, J. (1994). Inhibitory K^+ current activated by odorants in toad olfactory neurons. *Proc. R. Soc. Lond. B* **257**, 235–242.

MURROW, B. W., JAFEK, B. W. AND KINNAMON, S. S. (1995). Membrane currents in mammalian olfactory epithelium and vomeronasal organ receptor cells. *Chem. Senses* **19** (Abstract), 528.

NEHER, E. (1992). Correction for liquid junction potentials in patch clamp experiments. *Meth. Enzymol.* **207**, 123–131.

NEVITT, G. A. AND MOODY, W. J. (1992). An electrophysiological characterization of ciliated olfactory receptor cells of the coho salmon *Oncorhynchus kisutch*. *J. exp. Biol.* **166**, 1–17.

NGAI, J., DOWLING, M. M., BUCK, L., AXEL, R. AND CHESS, A. (1993). The family of genes encoding odorant receptors in the channel catfish. *Cell* **72**, 657–666.

OKADA, Y., TEETER, J. H. AND RESTREPO, D. (1994). Inositol 1,4,5-trisphosphate-gated conductance in isolated rat olfactory neurons. *J. Neurophysiol.* **71**, 595–602.

RAJENDRA, S., LYNCH, J. W. AND BARRY, P. H. (1992). An analysis of Na^+ currents in rat olfactory receptor neurons. *Pflügers Arch.* **420**, 342–346.

ROSSANT, J. AND HOPKINS, N. (1992). Of fin and fur: mutational analysis of vertebrate embryonic development. *Genes Dev.* **6**, 1–13.

RUDY, B. (1988). Diversity and ubiquity of K channels. *Neuroscience* **25**, 729–749.

SACCHI, O. AND BELLUZZI, O. (1993). The action potential in mammalian neurons: new perspectives. *News physiol. Sci.* **8**, 42–44.

SCHILD, D. (1989). Whole-cell currents in olfactory receptor cells of *Xenopus laevis*. *Exp. Brain Res.* **78**, 223–232.

SELMAN, K., PETRINO, T. R. AND WALLACE, R. A. (1994). Experimental conditions for oocyte maturation in the zebrafish, *Brachydanio rerio*. *J. exp. Zool.* **269**, 538–550.

SELMAN, K., WALLACE, R. A., SARKA, A. AND QI, X. (1993). Stages of oocyte development in the zebrafish, *Brachydanio rerio*. *J. Morph.* **218**, 203–224.

SHEPHERD, G. M. (1994). Discrimination of molecular signals by the olfactory receptor neuron. *Neuron* **13**, 771–790.

SILVER, W. L., CAPRIO, J., BLACKWELL, J. F. AND TUCKER, D. (1976). The underwater electro-olfactogram: a tool for the study of the sense of smell of marine fishes. *Experientia* **32**, 1216–1217.

STEELE, C. W., OWENS, D. W. AND SCARFE, A. D. (1990). Attraction of zebrafish *Brachydanio rerio* to alanine and its suppression by copper. *J. Fish Biol.* **36**, 341–352.

STEELE, C. W., SCARFE, A. D. AND OWENS, D. W. (1991). Effects of group size on the responsiveness of zebrafish *Brachydanio rerio* Hamilton Buchanan to alanine a chemical attractant. *J. Fish Biol.* **38**, 553–564.

STRÄHLE, U. AND BLADER, P. (1994). Early neurogenesis in the zebrafish embryo. *FASEB J.* **8**, 692–698.

STUART, G. W., VIELKIND, J. R., MCMURRAY, J. V. AND WESTERFIELD, M. (1990). Stable lines of transgenic zebrafish exhibit reproducible patterns of transgene expression. *Development* **109**, 577–584.

SUZUKI, N. (1977). Intracellular responses of lamprey olfactory receptors to current and chemical stimulation. In *Food Intake and Chemical Senses* (ed. Y. Katsuki, M. Sato, S. F. Takagi and Y. Oomura), pp. 13–22. Tokyo: University of Tokyo Press.

SUZUKI, N. (1989). Voltage- and cyclic nucleotide-gated currents in isolated olfactory receptor cells. In *Chemical Senses*, vol. 1, *Receptor Events and Transduction in Taste and Olfaction* (ed. J. Brand), pp. 469–493. New York: Marcel Dekker, Inc.

TROMBLEY, P. Q. AND WESTBROOK, G. L. (1991). Voltage-gated currents in identified rat olfactory receptor neurons. *J. Neurosci.* **11**, 435–444.

TROTIER, D. (1986). A patch-clamp analysis of membrane currents in salamander olfactory receptor cells. *Pflügers Arch.* **407**, 589–595.

TROTIER, D. AND MACLEOD, P. (1986). Intracellular recordings from salamander olfactory supporting cells. *Brain Res.* **374**, 205–211.

TSIEN, R. W., LIPSCOMBE, D., MADISON, D. V., BLEY, K. R. AND FOX, A. P. (1988). Multiple types of neuronal calcium channels and their selective modulation. *Trends Neurosci.* **11**, 431–438.

VAN DEN HURK, R. AND LAMBERT, J. G. D. (1983). Ovarian steroid glucuronides function as sex pheromones for male zebrafish, *Brachydanio rerio*. *Can. J. Zool.* **61**, 2381–2387.

VAN DEN HURK, R., SCHOONEN, W. G. E. J., VAN ZOELEN, G. A. AND LAMBERT, J. G. D. (1987). The biosynthesis of steroid glucuronides in the testis of the zebrafish *Brachydanio rerio* and their pheromonal function as ovulation inducers. *Gen. comp. Endocr.* **68**, 179–188.

VAUGHAN-JONES, R. D. AND AIKIN, C. C. (1995). Ion-selective electrodes. In *Microelectrode Techniques: the Plymouth Workshop Handbook* (ed. N. B. Standen, P. T. A. Gray and M. J. Whitaker), pp. 138–167. Cambridge: The Company of Biologists Limited.

WEAST, R. C. (1968). *Handbook of Chemistry and Physics*. Cleveland: The Chemical Rubber Co.

ZUFALL, F., FIRESTEIN, S. AND SHEPHERD, G. M. (1994). Cyclic nucleotide-gated ion channels and sensory transduction in olfactory receptor neurons. *A. Rev. biophys. biomolec. Struct.* **23**, 577–607.

ZUFALL, F., STENGL, M., FRANKE, C., HILDEBRAND, J. G. AND HATT, H. (1991). Ionic currents of cultured olfactory receptor neurons from antennae of male *Manduca sexta*. *J. Neurosci.* **11**, 956–965.